# Chapter 19

# Development of Novel Piezoelectric Biosensor Using PZT Ceramic Resonator for Detection of Cancer Markers

**Li Su, Chi-Chun Fong, Pik-Yuan Cheung, and Mengsu Yang**

## Abstract

A novel biosensor based on piezoelectric ceramic resonator was developed for direct detection of cancer markers in the study. For the first time, a commercially available PZT ceramic resonator with high resonance frequency was utilized as transducer for a piezoelectric biosensor. A dual ceramic resonators scheme was designed wherein two ceramic resonators were connected in parallel: one resonator was used as the sensing unit and the other as the control unit. This arrangement minimizes environmental influences including temperature fluctuation, while achieving the required frequency stability for biosensing applications. The detection of the cancer markers Prostate Specific Antigen (PSA) and α-Fetoprotein (AFP) was carried out through frequency change measurement. The device showed high sensitivity (0.25 ng/ml) and fast detection (within 30 min) with small samples (1 μl), which is compatible with the requirements of clinical measurements. The results also showed that the ceramic resonator-based piezoelectric biosensor platform could be utilized with different chemical interfaces, and had the potential to be further developed into biosensor arrays with different specificities for simultaneous detection of multiple analytes.

**Key words** Piezoelectric, Ceramic resonator, Prostate specific antigen, α-fetoprotein

## 1 Introduction

Biosensors are analytical devices composed of a recognition element coupled to a physical transducer, which can be very useful for on-site analysis of biomarkers. Different types of transducers have been used for biosensor development including optical, electrochemical, and piezoelectric transducers. The coupling of electrical and mechanical energy makes piezoelectric materials useful in a broad range of applications including energy conversion, sensors and actuators, and telecommunication [1]. There has been increasing interest in the use of piezoelectric devices as biosensors due to their attractiveness for applications in mass-sensitive detection and label-free analyses [2–4].

Piezoelectricity is derived from the Greek *piezo* or *piezein*, which means to squeeze or press. It is the coupling between a

Ben Prickril and Avraham Rasooly (eds.), *Biosensors and Biodetection: Methods and Protocols, Volume 2: Electrochemical, Bioelectronic, Piezoelectric, Cellular and Molecular Biosensors*, Methods in Molecular Biology, vol. 1572,
DOI 10.1007/978-1-4939-6911-1_19, 

material's mechanical and electrical behaviors in noncentrosymmetric crystals. When applying a stress, an electric polarization or charge will be induced in such a material, which can be recorded as a sensing signal. Various piezoelectric materials have been used in piezoelectric biosensors development such as piezoelectric nanogenerators [5] and piezoelectric polymer diaphragms [6]. However, the most conventional piezoelectric materials are quartz crystals and the synthetic polycrystalline ferroelectric ceramics such as lead titanate zirconate (PZT). Normally piezoelectric biosensors are mass sensitive detectors that use an oscillating piezoelectric resonator as the transducer. Coating the resonator with biological materials results in high selectivity for target molecules such as antibodies or enzymes [7]. The sensing mechanism is based on mass changes due to reactions involving target molecules bound to the transducer surface. The signals are normally easily detectable by measuring the fundamental frequency variations of piezoelectric oscillators [8, 9].

Quartz crystals are the most well-known piezoelectric materials. In 1959, Sauerbrey first described the dependence of the resonance frequency of a piezoelectric quartz crystal on the mass change due to surface deposition [10]. Quartz crystals have been widely used as the so-called quartz crystal microbalance (QCM) in surface science and industry. Biosensors based on quartz crystal transducers for the detection of DNA, proteins, viruses, bacteria, and toxins in living cells [11] have been developed and applied in food, biochemical, environmental and clinical analyses, as well as for detection of various hydrocarbons [12], pollutants [13, 14], and gas-phase analytes [15]. Numerous combinations of piezoelectric quartz crystal devices with immunological elements have been reported [13, 16–18]. However, as the sensitivity of piezoelectric biosensors depends on the oscillating frequency as well as the area and thickness of the material, there are technical difficulties in producing thinner, smaller quartz with higher frequency. These physical barriers place a limit on the application of quartz crystal biosensors with regard to sensitivity and cost.

Synthetic polycrystalline ferroelectric ceramics such as PZT also represent piezoelectric materials with applications as conventional industrial electronic products. They have been used as the substrates of piezoelectric igniters, transducers, transformers, electric resonators, speakers, filters, and ultrasonic motors [19]. The technology of manufacturing stable, high frequency (10–100 MHz range) ceramic material is mature and these materials are readily available. Investigations of PZT piezoelectric ceramics on surface acoustic wave (SAW) applications [20, 21], materials properties [22], and electrical characteristics [23] have been reported. Both resonant piezo-layers of screen printed PZT film [24] and bulk PZT in the form of discs with gold electrodes [25] have been utilized in mass sensor development. However, previously there

were very limited applications of piezoelectric ceramic materials, where the piezoelectric ceramic resonators employed had very low resonant frequency (less than 200 kHz) and narrow detection range (100–700 Hz) [25–27]. Ceramic resonators are easily mass produced with low cost and have the advantages of mechanical ruggedness, small size, ease of fabrication in complex shapes, and flexibility with higher resonance frequencies. Although the precision of frequency control in ceramic resonators is reduced when compared to quartz crystal resonators, the above properties make them suitable for biosensor development.

We have developed a piezoelectric biosensor platform for label-free, cost-effective, and direct detection of biomarkers such as prostate specific antigen (PSA), α-fetoprotein (AFP), and endocrine disrupting chemicals (EDCs) by using commercially available PZT ceramic resonators [7, 28]. The sensing mechanism is also based on direct absolute mass resonance sensing. This biosensor platform may be further multiplexed to incorporate miniaturized sensor arrays with different specific antibodies for detection of multiple analytes in parallel.

This investigation involves four major steps: (1) theoretical property study of piezoelectric ceramic resonators, (2) material investigation and optimization of piezoelectric ceramic resonators, (3) parallel-connected (dual) ceramic resonators scheme design, and (4) biosensor development based on a dual resonator chip. Different surface chemistry methods for immobilization of antibody onto sensor surfaces were investigated and different interfaces, including protein A and nafion for antibody immobilization, were successfully developed. Detection of selected cancer biomarkers such as prostate specific antigen (PSA) and α-fetoprotein (AFP) were carried out to evaluate the performance of the biosensor, which showed high sensitivity (0.25 ng/ml) and fast detection (within 30 min).

## 2 Materials

### 2.1 Apparatus

1. Gold-plated ceramic resonators with different frequencies (40, 50, and 70 MHz) were obtained from Murata Manufacturing Co., Ltd. (Japan). The ceramic wafer had gold plated electrodes on both sides and the dimension of the ceramic wafer is 2 mm × 1.6 mm × 0.55 mm. The PZT has a formula of Pb$\alpha$-$a$Mea[(MII1/3MV(2 + $b$)/3)zTixZr1 − $x$− $z$]O3, wherein Me represents a metal element; MII represents an acceptor element of a divalent metal element; MV represents a donor element of a pentavalent metal element; and $z$, $b$, $x$, $\alpha$, and $a$ satisfy $0.05 \leq z \leq 0.40$, $0 < bz/3 \leq 0.035$, $0.345 \leq x \leq 0.480$, $0.965 \leq \alpha \leq 1.02$, and $0 \leq a \leq 0.05$ (parameters from the manufacturer).

2. Frequency detection equipment: Impedance Analyzer (IA) from Hewlett Packard (4195A) with a detection range of 10 Hz–500 MHz (*see* **Note 1**).
3. A plasma cleaner (model: PDC-3xG) was from HARRICK for ceramic surface cleaning.

### 2.2 Reagents

1. Protein A was obtained from Sigma Chemical Co. (St Louis, MO) (*see* **Note 2**).
2. Bovine serum albumin (BSA) was purchased from Bio-Rad Laboratories (Rockville Center, NY).
3. AFP antigen, PSA, and human CRP were obtained from Calbiochem (La Jolla, CA) (*see* **Note 3**).
4. AFP antibody and PSA antibody were from GeneTex, Inc. (San Antonio, Texas) (*see* **Note 3**).
5. Nafion (perfluorinated ion-exchange resin, 5 %, w/v solution) was obtained from Aldrich.
6. The potassium phosphate/sodium phosphate were from Sigma for preparation of phosphate buffered saline (PBS, 50 mM, pH 7.4).

## 3 Methods

### 3.1 Theoretical Property Study of Piezoelectric Ceramic Resonators

The theoretical mass sensitivity of the ceramic resonator was calculated and compared to quartz crystal. Since the most commonly used piezoelectric biosensors were based on 5–10 MHz quartz crystal resonators, a 10 MHz quartz crystal (QC) resonator was selected to compare with the 40 MHz ceramic resonator used in this study.

The resonance frequency is related to thickness of the ceramic wafer:

$$f = \frac{N}{t} = \frac{\rho}{m} N \tag{1}$$

Where $f$ (Hz) is the fundamental resonance frequency, $N$ (cm Hz) is the frequency constant, $t$ is the wafer thickness (cm), $\rho$ (g cm$^{-3}$) is the density, and m (g cm$^{-2}$) is the area density of mass.

Assuming the deposited mass $\Delta m$ (g) is evenly distributed on the wafer surface and the frequency will change accordingly:

$$f + \Delta f = \frac{\rho N}{m + \Delta m/A} \tag{2}$$

Substituting Eqs. 1 into 2 leads to:

$$\Delta f = -\frac{f^2}{\rho N} \times \frac{\Delta m/A}{1 + \frac{\Delta m/A}{m}} \tag{3}$$

When $\Delta m << m$, and $\frac{\Delta m/A}{m} \approx 0$, Eq. 3 yields

$$\Delta f = -\frac{f^2}{\rho N} \times \frac{\Delta m}{A} = -\frac{f^2}{AN\rho} \times \Delta m \tag{4}$$

As for ceramic resonators, the density ($\rho$) and frequency constant ($N$) are 7.54 g/cm$^3$ and 7.85 $\times$ 10$^5$ cm Hz respectively (parameters from the manufacturer). By substituting these values into Eq. 4, the sensitivity calculation equation for the ceramic resonators should be:

$$\Delta f = -1.69 \times 10^{-7} \times f^2 \times \frac{\Delta m}{A} \tag{5}$$

The sensing surface area ($A$) of the 40 MHz ceramic resonator used in this study is 0.39 mm$^2$. Therefore, the sensitivity of this material is 69.3 Hz/ng. The theoretical calculations for quartz crystal are based on the Sauerbrey equation [10] and the sensitivity calculation of 10 MHz QC with 50.2 mm$^2$ electrode area [29] is 0.45 Hz/ng. This indicates that ceramic resonators with higher resonance frequency and smaller size may give higher sensitivity. On the other hand, ceramic resonators are more sensitive to temperature, humidity, and other environmental influences, resulting in higher background noise than that for quartz crystal resonators.

Table 1 presents a detailed comparison between 10 MHz quartz crystal resonators and 40 MHz piezoelectric ceramic resonators, including vibration mode, temperature coefficient, cost, and size. Firstly, ceramic resonators, which are usually operated under thickness extension mode, exhibit much higher oscillation frequency (1–100 MHz) than quartz crystal resonators, which are often operated under thickness shear mode (1–10 MHz) [7]. Secondly, thermal stability is a key parameter required for commercial applications. The temperature coefficient of a piezoelectric resonator is dependent on material properties as well as the

**Table 1**
**Comparison of ceramic resonators with quartz crystal resonators**

| Name | Oscillation frequency (MHz) | Vibration mode | Temperature coefficient | Price /$USD | Wafer area / mm$^2$ | Electrode area/mm$^2$ | Long-term stability |
|---|---|---|---|---|---|---|---|
| Ceramic resonator | 40 | Thickness extension (TE) | $\leq 10^{-5}$/°C | ~0.5 | 3.2 | 0.37 | Excellent |
| Quartz crystal | 10 | Thickness shear (TS) | $\leq 10^{-6}$/°C | ~10 | 153.8 | 50.2 | Excellent |

dimension and vibration mode of the resonator [30]. Since PZT is a polycrystalline material but quartz is a crystalline material, the temperature coefficient of ceramic resonators is much greater than quartz crystal resonators, which indicates that ceramic resonators are more sensitive to temperature fluctuations and have a less stable resonant frequency. Changing the composition of a piezoelectric ceramic may improve the thermal stability [31, 32]. Moreover, it is easier to produce thinner and smaller ceramic resonators which are much lower cost than quartz resonators.

### 3.2 Material Investigation and Optimization of Piezoelectric Ceramic Resonators

Since there has been limited research on piezoelectric ceramic biosensor development, properties of ceramic resonators need to be evaluated thoroughly first. Commercially available high frequency ceramic resonators (40, 50, 70 MHz) were tested by connecting them to an Impedance Analyzer as shown in Fig. 1. The piezoelectric ceramic resonator chip comprises a "sandwich" structure composed of a ceramic wafer interposed between two layers of gold electrode (Fig. 1a). The gold electrodes are used to connect the ceramic wafer with an external oscillation circuit or an impendence analyzer, which causes the ceramic resonator to vibrate under resonance frequency. The gold surface serves as a support for immobilization of antibodies or other biomaterials for biosensor development.

1. Stability of PZT ceramic resonators with different frequencies (40, 50, and 70 MHz) were evaluated first within 30 min at 25.0 °C as shown in Fig. 2a. It was shown that the 40 MHz ceramic resonators generate about a 3.75 ppm frequency shift, which is smaller than those of 50 MHz (5 ppm) and 70 MHz (5.7 ppm) ceramic resonators. This indicates that the 40 MHz

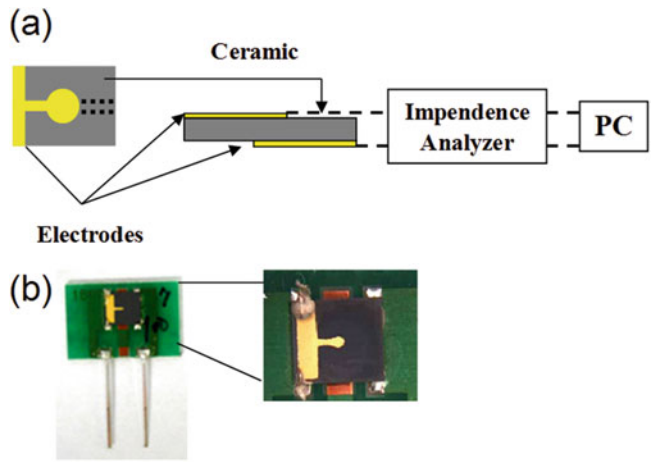


**Fig. 1** (**a**) Schematic layout of the ceramic resonator and the measurement system; (**b**) Photo of a 40 MHz ceramic resonator

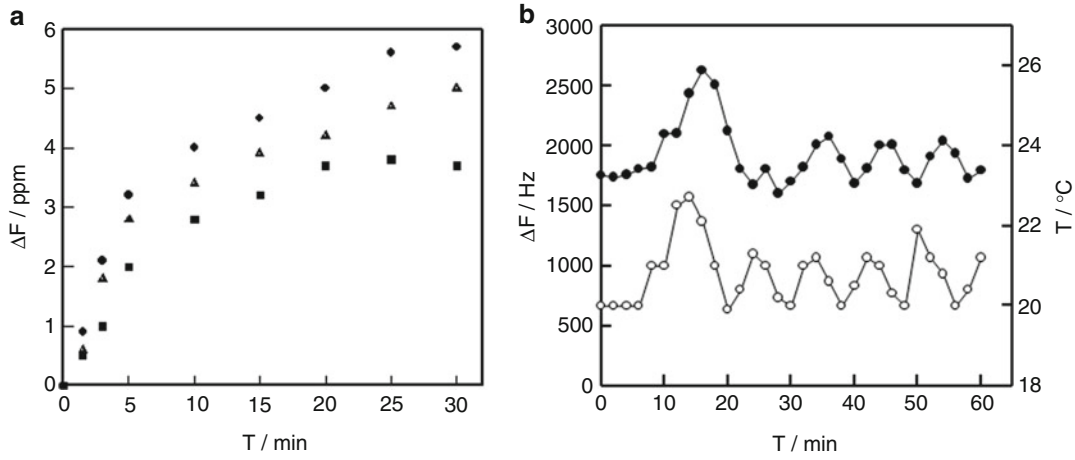


**Fig. 2** (**a**) Stability evaluation of ceramic resonators at different resonance frequencies within 30 min at 25.0 °C (*filled circle* for 70 MHz resonator; *filled triangle* for 50 MHz resonator and *filled square* for 40 MHz resonator): percentage of frequency shift; (**b**) Frequency shift (*filled circle*) of a 40 MHz ceramic resonator with environmental temperature fluctuation between 20 and 22 °C (*open circle*)

ceramic resonators are more stable than 50 and 70 MHz ones, and should be the preferred choice for biosensor development.

2. The stability of the 40 MHz ceramic resonators was further studied under different temperature conditions. The frequency change of a 40 MHz ceramic resonator was measured for 60 min while the ambient temperature was raised from 20 to ~22 °C. A shielding metal box was placed outside the resonator to eliminate other possible environment influences such as radio waves. As shown in Fig. 2b, the frequency change paralleled the room temperature change with a time delay (~2 min) due to delayed heat transfer through the surrounding metal box. A large frequency shift (~450 Hz/°C) was detected which corresponds to a temperature coefficient of $10^{-5}$ Hz/°C.

### *3.3 Parallel-Connected (Dual) Ceramic Resonators Scheme Design*

Due to large frequency shifts induced by environmental influences, a (dual) resonator using a parallel connection scheme was developed to compensate for the shifts, as shown in Fig. 3. In the dual design scheme, two 40 MHz ceramic resonators (the so-called two channels) were connected in parallel to an Impedance Analyzer and placed in a shielding metal box for frequency measurement. As the two resonators are under the same environment, one of them can serve as reference and the other one for sample measurement to reduce environmental interferences. One of the problems encountered for this design was how to avoid the interference between the parallely connected resonators due to their close proximity. High frequency resonators at the same frequency level (e.g., 40 MHz piezoelectric ceramic resonators used in this study) may have cross talk between each other when they are oscillating at the same time.

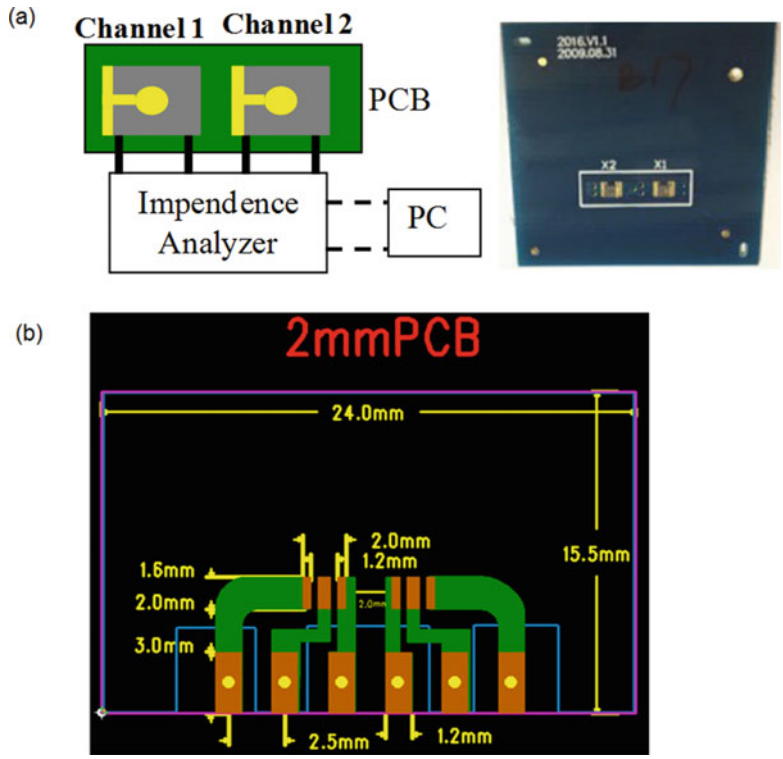


**Fig. 3** (**a**) Schematic layout of dual ceramic resonators and the measurement system (*left*) and photo of a ceramic resonator (*right*); (**b**) Dimensions of the electrode leads and connections on the printed circuit board for dual ceramic resonators

As shown in Fig. 4, ceramic resonators with resonance frequencies that are close in value (e.g., $\Delta F = 30$ kHz) are subject to large interference, resulting in a large effect on the frequency reading. By increasing $\Delta F$ the interference will be reduced or even eliminated. We have tested resonator pairs with various $\Delta F$ values in order to identify a desirable threshold. As indicated in Fig. 5, when the resonance frequency difference between the resonators was greater than ~100 kHz, the interference between the resonators could be eliminated. Thus a minimum resonance frequency difference ($\Delta F$) of 100 kHz was adopted in the following biosensor development.

The feasibility of using this parallel-connected resonator design to compensate for the large frequency change induced by environmental influences was tested. Two resonators were connected in parallel and their frequency readings were simultaneously recorded for 30 min. The environmental temperature shifted about 1° during this period.

As shown in Fig. 5, the frequencies of both individual resonators were changed and the shift trends are similar. For line 1 this frequency is ~450 Hz and for line 2 ~400 Hz. The frequency shift difference ΔF is only about 130 Hz (line 3). These results indicate

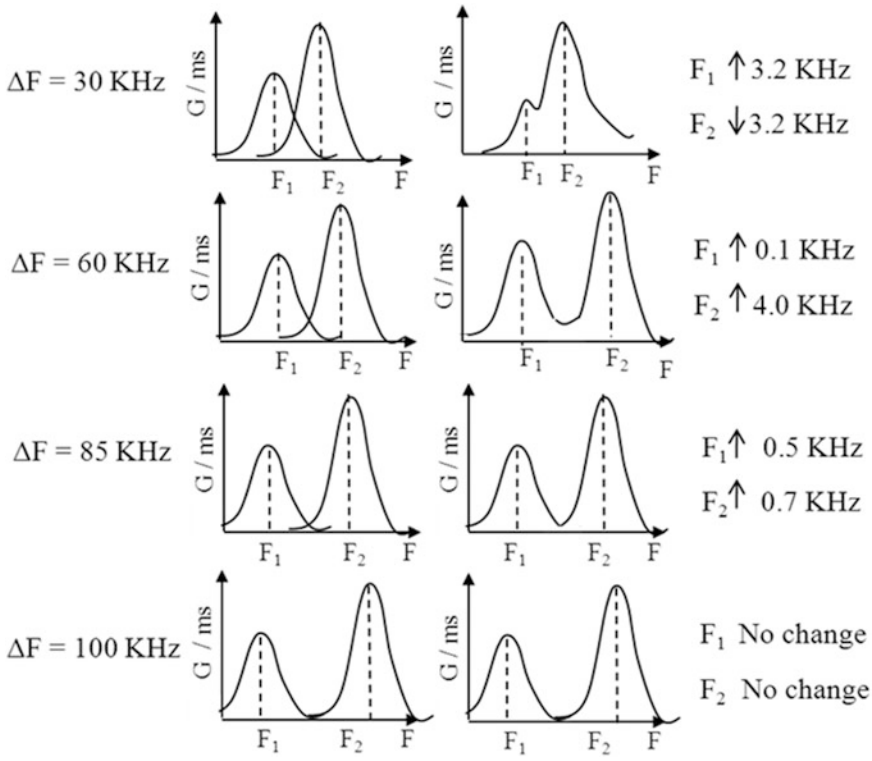


**Fig. 4** Frequency (*F*) in kHz and conductance (*G*) in m s (m sigma) change before and after parallel connection of two ceramic resonators with different resonance frequencies were recorded at 25 °C

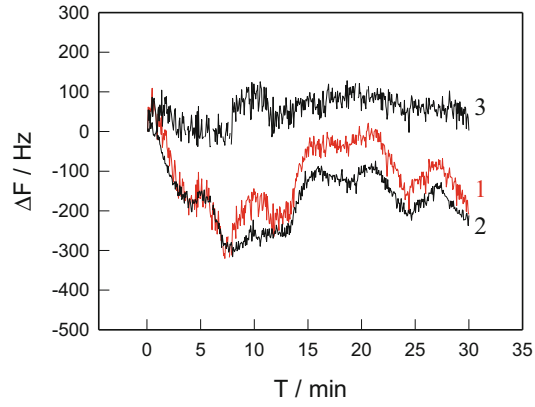


**Fig. 5** Frequency shift Δ*F* of two parallel connected 40 MHz resonators (*line 1* and *line 2*) and frequency shift difference between these two resonators (*line 3*) within 30 min when the environmental temperature shifts about 1 °C (from 25 to 26 °C)

that parallel connection of the resonators can reduce the frequency shift under ambient conditions. The experiment was repeated several times on different pairs of parallelly connected resonators and the frequency difference shifts are all below 150 Hz. Thus the parallel connection design of the ceramic resonators was adopted in developing the biosensor, and the noise level was set to 150 Hz for purposes of sample analysis.

### 3.4 Biosensor Development Based on Dual Resonator Chip

Antibody immobilization is a vital step in a successful development of piezoelectric biosensors. An effective and easy-to-use biosensor platform should accommodate varied chemical protocols and work with a variety of biological applications. For example, specific chemical interfaces should be selectable for detection of different biomarkers. In this chapter we choose to evaluate immobilization using Protein A and nafion.

#### 3.4.1 Protein A Method

Protein A was used as a linker for antibody immobilization because it can form a strong complex ($K_a = 10^8$ l/mol) with a gold electrode surface by physical adsorption due to its affinity toward the Fc region of the IgG molecule [33]. As shown in Fig. 3, there are two channels (ceramic resonators) per sensor chip. The operating steps are as follows:

1. Ceramic surfaces were cleaned by using a plasma cleaner for 5 min at 400 MV with 400 ml oxygen or Ar gas.
2. Protein A was then used as a linker group to modify the resonator surface. 1 μl of a 2 mg/ml protein A solution was spread onto the cleaned gold surface and incubated for 24 h.
3. After incubation the gold surface was washed with deionized water and dried under $N_2$, prior to antibody immobilization (*see* **Note 4**).
4. After Protein A incubation, one channel was immobilized with PSA antibody, while PBS buffer was applied instead of antibody solution on the other channel as reference: 1 μl of antibody solution (1 mg/ml), PSA antibody was added to the modified ceramic resonator surface and incubated for 1 h at room temperature, followed by incubation with 3 % BSA for 2 h to block nonspecific binding sites. After washing and drying, the biosensor was ready for antigen detection (*see* **Note 5**).
5. PSA antigens at different concentrations (0.25, 2.5, 25, $2.5 \times 10^2$, $2.5 \times 10^3$ ng/ml) were added to both channels in series and incubated for 1 h.
6. The detection signal was recorded as frequency change using an Impedance Analyzer (IA) after applying antigen solution, and plotted against the log concentration of antigen as shown in Fig. 6 (*see* **Note 6**).

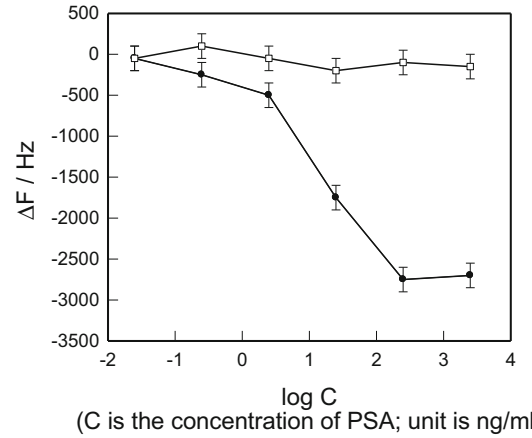


**Fig. 6** Frequency changes against the log concentration of the PSA. PSA detection plot (*filled circle*) vs. PBS control plot (*open circle*). The concentrations of PSA solutions are 0.025, 0.25, 2.5, 25, $2.5 \times 10^2$, $2.5 \times 10^3$ ng/ml

As shown in Fig. 6, the antibody–antigen interaction led to specific frequency shifts as compared to the PBS control. Moreover, the biosensor exhibits a high sensitivity, with a PSA detection range from 2.5 ng/ml to $2.5 \times 10^2$ ng/ml, with saturation at $2.5 \times 10^2$ ng/ml. This sensitivity is comparable to that required for clinical measurement; PSA levels are normally below 4 ng/ml with a threshold level of 10 ng/ml [34]. These results demonstrate that the piezoelectric ceramic resonator biosensor is an effective transducer of for sensitive detection of biomarkers.

### 3.4.2 *Nafion Method*

Nafion is a sulfonated tetrafluoroethylene based fluoropolymer. It is ionomers formed by synthetic polymers with ionic properties. It is hydrophilic, nonelectroactive and chemically inert, possessing almost ideal characteristics for modification of electrodes [16]. The thickness of nafion film is an important element that influences the performance of the immunoassay. Previous investigations have shown that a 1 % nafion coating solution was optimal for preparation of nafion-modified electrodes [9, 16, 35, 36]. Hence this concentration was adopted in our study. The operating steps are the following:

1. Ceramic surfaces were cleaned using a plasma cleaner for 5 min at 400 MV with 400 ml oxygen or Ar gas.
2. 1 % Nafion coating solution was prepared by diluting the 5 % Nafion stock solution in 10 % ethanol (v/v) in DDW.
3. 0.5 μl of 1 % Nafion coating solution was spread onto the cleaned gold electrode surface and dried at room temperature.
4. The gold surface was washed by deionized water and dried under $N_2$.

**Table 2**
**The frequency changes of the binding of PSA (2 ng/ml) to PSA antibody-immobilized resonator (detection channel) or control channel (without PSA antibody) at 4 min and 1 h were compared**

| PSA detection channel | $\Delta F$ (Hz) | PBS control channel | $\Delta F$ (Hz) |
|---|---|---|---|
| 2 ng/ml PSA 4 min | −500 | 2 ng/ml PSA 4 min | 40 |
| 2 ng/ml PSA 1 h | −300 | 2 ng/ml PSA 1 h | −160 |
| Total signal | −800 | Total signal | −120 |

5. 1 μl of 1 mg/ml antibody solution, AFP antibody or PSA antibody (PBS buffer was applied to the reference) was added onto the modified ceramic resonator surface and incubated for 1 h at room temperature, followed by incubation with 3 % BSA for 2 h to block nonspecific binding sites. After washing and drying the biosensor was ready for antigen detection (*see* **Note 5**).
6. 1 μl of AFP or PSA (in PBS) solution at different concentrations were spread onto the biosensor surface and incubated for 1 h to allow antibody–antigen interaction. After incubation, the surface was washed by deionized water and dried under $N_2$ (*see* **Note 5**).
7. The frequency change was detected before and after applying antigen by IA (*see* **Note 6**).

In the control test, one channel was immobilized with PSA antibody, while the other acted as a control to evaluate the nonspecific binding. As shown in Table 2, when 1 μl of 2 ng/ml PSA solution was added to both channels and incubated for 1 h, the antigen binding to the antibody-immobilized resonator (the detection channel) caused a frequency drop of −800 Hz, which was much larger than that of the control channel (−160 Hz). Even during the first 4 min, there was a binding signal on the detection channel ($\Delta F = -500$ Hz), while the reference channel resulted in a 40 Hz frequency drop. Therefore, the detection time could be shortened based on the binding kinetics.

The feasibility of detecting two cancers markers by the dual resonator biosensor was also tested by immobilizing two different antibodies on the two channels respectively as shown in Fig. 7. The AFP marker and its antibody were included here. During the test, one channel was immobilized with PSA antibody and the other channel was immobilized with AFP antibody. As shown in Fig. 8, there was a specific binding signal with a frequency drop of −1400 Hz on the PSA antibody immobilized channel when applying 1 μl of 10 ng/ml PSA solution to both channels, while the AFP immobilized channel only resulted in a 120 Hz frequency decrease,

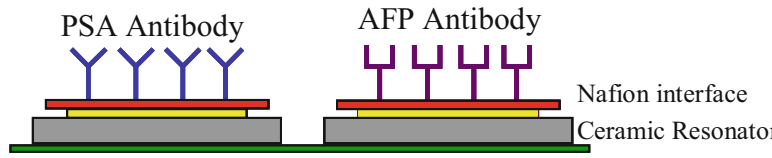


**Fig. 7** Illustration of PSA antibody and AFP antibody immobilization on the two channels of ceramic resonators respectively

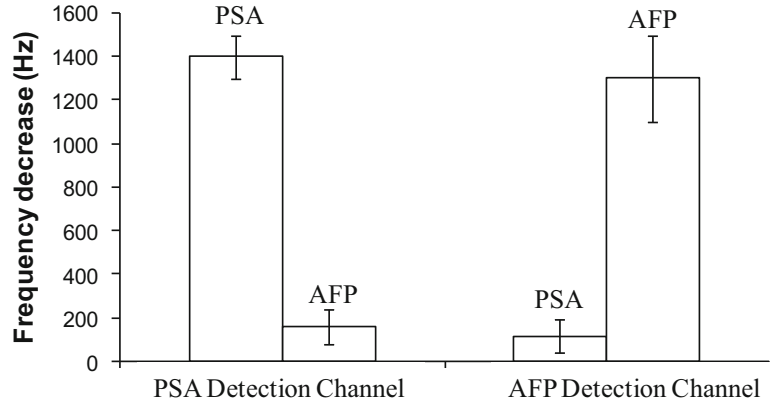


**Fig. 8** Specific antigen binding evaluation on PSA and AFP detection channels, where the PSA and AFP solutions are 10 ng/ml and 1 μg/ml respectively

which was within the noise level threshold. In contrast, when applying AFP antigen solution the AFP detection channel gave a much stronger signal than the PSA channel. Similarly, when 1 μl of 1 μg/ml AFP solution was added to both channels the AFP channel recorded a −1270 Hz frequency shift while the PSA channel recorded a −94 Hz shift, indicating the specificity of the biosensor.

It was demonstrated that two different antibodies could be successfully immobilized onto the ceramic surface and the specific antigen could be detected accordingly. By simply adding one reference (control) chemical, the sensor system could detect two biomarkers in parallel. In principal array ceramic resonator biosensor chips can be used to detect many other biomarkers.

## 4 Notes

1. An external oscillation circuit can be used instead of an impedance analyzer.
2. All chemicals used were of analytical grade unless otherwise stated.

3. Two kinds of "antibody–antigen" pairs were used in this study, whereas numerous other reagents are available from other commercial sources.
4. Deionized water (resistivity >18 MΩ cm) was used throughout the experiments.
5. The modified resonators could be stored in a refrigerator for a few days, but need to be brought to room temperature before carrying out the next step.
6. The frequency signals at every on-chip reaction step must be monitored.

## References


1. Setter N (2002) Piezoelectric materials in devices, Ceramics Laboratory, EPFL, Switzerland
2. Ward MD, Buttry DA (1991) In situ interfacial mass detection with piezoelectric transducers. Science 249:1000–1007
3. Suleiman AA, Guilbault GG (1994) Recent developments in piezoelectric immunosensors. A review. Analyst 119:2279–2282
4. Bizet K, Gabrielli C, Perrot H (1999) Biosensors based on piezolectric transducers. Analusis 27(7):609–616
5. Zhao YY, Fu YM, Wang PL et al (2015) Highly stable piezo-immunoglobulin-biosensing of a $SiO_2$/ZnO nanogenerator as a self powered/active biosensor arising from the field effect influenced piezoelectric screening effect. Nanoscale 5(7):1904–1911
6. Lu X, Guo QS, Xu Z et al (2015) Biosensor platform based on stress-improved piezoelectric membrane. Sensor Actuator 179:32–38
7. Su L, Zou L, Fong CC et al (2013) Detection of cancer biomarkers by piezoelectric biosensor using PZT ceramic resonator as the transducer. Biosens Bioelectron 46:155–161
8. Babacan S, Pivarnik P, Letcher S et al (2000) Evaluation of antibody immobilization methods for piezoelectric biosensor application. Biosens Bioelectron 15:615–621
9. Susmel S, Toniolo R, Pizzariello A et al (2005) A piezoelectric immunosensor based on antibody entrapment within a non-totally rigid polymeric film. Sensor Actuator 111–112:331–338
10. Sauerbrey GZ (1959) Verwendung von Schwingquarzen zur Wägung dünner Schichten und zur Mikrowägung. Z Phys 155:206–222
11. Marx KA (2003) Quartz crystal microbalance: a useful tool for studying thin polymer films and complex biomolecular systems at the solution−surface interface. Biomacromolecules 4(5):1099–1120
12. Percival CJ, Stanley S, Galle TM et al (2001) Molecular-imprinted, polymer-coated quartz crystal microbalances for the detection of terpenes. Anal Chem 73(17):4225–4228
13. Su X, Chew FT, Li SF (2000) Piezoelectric quartz crystal based label-free analysis for allergy disease. Biosens Bioelectron 15 (11–12):629–639
14. Yao C, Qi Y, Zhao Y et al (2009) Aptamer-based piezoelectric quartz crystal microbalance biosensor array for the quantification of IgE. Biosens Bioelectron 24(8):2499–2503
15. Zhang Y, Lin F, Zhang Y et al (2011) Quartz crystal microbalance detection of DNA single-base mutation based on monobase-coded cadmium tellurium nanoprobe. Anal Sci 27 (12):1229–1235
16. Deng T, Li JS, Wang H et al (2005) Piezoelectric immunoassay for complement C4 based on a Nafion-modified interface for antibody immobilization. J Immunol Methods 299 (1–2):1–8
17. Soumetz FC, Pastorino L, Ruggiero C (2009) Development of a piezoelectric immunosensor for matrix metalloproteinase-1 detection. Conf Proc IEEE Eng Med Biol Soc 2009:2775–2778
18. Yuan JB, Tan YG, Nie LH, Yao SZ (2002) Piezoelectric quartz crystal sensors based on ion-pair complexes for the determination of cinchonine in human serum and urine. Anal Chim Acta 454:65–74
19. Lee GM, Kim BH (2005) Effects of thermal aging on temperature stability of $Pb(Zr_yTi_{1-y})O_3$ + x(wt.%)$Cr_2O_3$ ceramics. Mater Chem Phys 91:233–236
20. Gualtieri JG, Kosinski JA, Ballato A (1994) Piezoelectric materials for acoustic wave

applications. IEEE Trans Ultrason Ferroelectr Freq Contr 41:53–59

21. Feuillard G, Lethiecq M, Janin Y, Tessier L, Pourcelot L (1997) Comparative performance of piezoceramic and crystal SAW filters. IEEE Trans Ultrason Ferroelectr Freq Contr 44:194–197
22. Lee PCY, Yu JD, Li X, Shih WH (1999) Piezoelectric ceramic disks with thickness-graded material properties. IEEE Trans Ultrason Ferroelectr Freq Contr 46:205–215
23. Kwork KW, Chan HLW, Choy CL (1997) Evaluation of the material parameters of piezoelectric materials by various methods. IEEE Trans Ultrason Ferroelectr Freq Contr 44:733–742
24. Ferari V, Marioli D, Taroni A et al (2000) Multisensor array of mass microbalances for chemical detection based on resonant piezolayers of screen-printed PZT. Sens Actuators B 68:81–87
25. Verissimo MIS, Mantas PQ, Senos AMR et al (2003) Suitability of PZT ceramics for mass sensors versus widespread used quartz crystals. Sens Actuators B 95:25–31
26. Eklund A, Backlund T, Lindahl OA (2000) A resonator sensor for measurement of intraocular pressure—evaluation in an in vitro pig-eye model. Physiol Meas 21:355–367
27. Lee JH, Hwang KS, Park J, Yoon KH et al (2005) Immunoassay of prostate-specific antigen (PSA) using resonant frequency shift of piezoelectric nanomechanical microcantilever. Biosens Bioelectron 20(10):2157–2162
28. Hu LS, Fong CC, Zou L et al (2014) Label-free detection of endocrine disrupting chemicals by integrating a competitive binding assay with a piezoelectric ceramic resonator. Biosens Bioelectron 53:406–413
29. Tang AXJ, Pravda M, Guilbault GG et al (2002) Immunosensor for okadaic acid using quartz crystal microbalance. Anal Chim Acta 471:33–40
30. Erhart J, Rusin L, Seifert L (2007) Resonant frequency temperature coefficients for the piezoelectric resonators working in various vibration modes. J Electroceramics 19:403–406
31. Lee JH, Yoon KH, Hwang KS et al (2004) Label free novel electrical detection using micromachined PZT monolithic thin film cantilever for the detection of C-reactive protein. Biosens Bioelectron 20(2):269–275
32. Lente MH, Zanin AL, Vasiljevic J et al (2004) Temperature coefficient of piezoelectric constants in Pb(Mg1/3 Nb2/3)O3–PbTiO3 ceramics. Mater Res 7:369–372
33. Deshpande SS (1996) Antibodies: biochemistry, structure, and function. In: Enzyme immunoassays: from concept to product development. Chapman and Hill, New York, pp 24–51
34. Ilic D, Forbes KM, Hassed C (2011) Lycopene for the prevention of prostate cancer. Cochrane Database Syst Rev 11:CD008007
35. Zhou YM, Wu ZY, Shen GL, Yu RQ (2003) An amperometric immunosensor based on Nafion-modified electrode for the determination of *Schistosoma japonicum* antibody. Sens Actuators B 89:292–298
36. Chetcuti AF, Wong DKY (1999) An indirect perfluorosulfonated ionomer-coated electrochemical immunosensor for the detection of the protein human chorionic gonadotrophin. Anal Chem 71:4088–4094